DOI: http://dx.doi.org/10.30684/etj.37.10A.9

Zena A. Salman
Materials Engineering Department, University of Technology, Baghdad, Iraq
zena_eng87@yahoo.com

Farhad M. Othman
Materials Engineering Department, University of Technology, Baghdad, Iraq

Alaa A. Abdul-hamed
Materials Engineering Department, University of Technology, Baghdad, Iraq

Received on: 19/04/2019
Accepted on: 17/05/2019
Published online: 25/10/2019

Structural and Morphological Investigation of Cr_2O_3/WO_3 Oxides Films Composite Using Modified Spray Pyrolysis Technique

Abstract-*Cr_2O_3/WO_3 oxides film composite was successfully synthesized via advanced controlled chemical spray pyrolysis deposition technique using two nozzles. Two solutions of tungstic acid and chromium chloride was sprayed separately at various ratios of (W: Cr) at the same time on a silicon substrate at 500 °C, the film then heat-treated at 400 °C for the 60s. The crystal structure, microstructure and morphology properties of prepared films were studied. Based on characterization techniques, crystallized Cr_2O_3/WO_3 mixed oxides films were investigated by X-ray diffraction after the annealing process, with film thickness of about 500 nm. The SEM and AFM revealed that rough and porous microstructures of Cr_2O_3/WO_3 were formed. The obtained microstructure has been known as one of the most effective microstructures due to having high surface area particularly in gas detection applications*

Keywords- *Cr_2O_3-WO_3, Thin film, Advance spray pyrolysis method, Microstructure characterization.*

How to cite this article: Z.A. Salman, F.M. Othman and A.A. Abdul-hamed, "Structural and Morphological Investigation of Cr_2O_3/WO_3 Oxides Films Composite Using Modified Spray Pyrolysis Technique," *Engineering and Technology Journal*, Vol. 37, Part A, No. 10, pp. 435-441, 2019.

1. Introduction

Tungsten and chromium oxides received considerable attention due to their superior action in various areas, such as environmental purification, dye-sensitized solar cells, and gas sensor [1]. The control of semiconductor composition, morphology, and microstructure are required for improving the characteristic of different oxides [2]. Mixed oxides can be classified into two categories: the main classification includes those that form particular chemical components such as $ZnSnO_3$ and Zn_2SnO_4. The second classification falls those blended oxides that compose solid solutions e.g., SnO_2-TiO_2, which is useful for gas sensing purposes and conductive electrodes [3]. For the approaches varying materials' properties, the user of the composite materials is an adequate selection to enhance the sensitivity of the gas sensors of metal oxide because they produce an effect more significant than the sum of their individual effects [4].

The general conception employs a combination of p and n-type semiconducting oxides for sensor applications [5] as for Cr_2O_3 used to improve the sensors based on WO_3. As reported by previous work, porous films of Cr_2O_3/WO_3 composite exhibits an excellent acetone sensing response. Another study reported that the sensor of Cr_2O_3/WO_3 with a hierarchical structure exhibits a great response to xylene gas, these above results indicate that the morphology of Cr_2O_3/WO_3 composite have a significant impact on gas sensing characteristics [6].

Numerous oxide blends can be custom fitted to accomplish wanted surface/volume proportions and microstructure to achieve different gas detecting efficiencies. When adding another component, a decreasing in grain size may happen, which likewise enhances gas sensor reaction properties [7]. Mixing of metal oxides in a sensor layer has lately been investigated to enhance sensor efficiency and thermal stability. The mixed oxides profit by the best detecting properties of their unmixed oxides, by altering the electronic structure of the oxides and lead to modify both the mass and surface characteristics [8].

Recently, various morphologies of metal oxide semiconductor (MOS) nanostructures for examples like wire, belt, and bar and tetra-units have been broadly explored for gas detecting applications. It is notable that the detecting property of these sensors emphatically depends on the microstructure and surface morphology of MOS mainly; 1D-dimensional nanostructures, for example, wires, belts, and needles that have obtained great attention in numerous synthesis and design of nanodevice [9, 10]. It is essential that the affectability of substance gas sensors is unequivocally influenced by the particular surface of detecting materials. A higher particular surface of a detecting material prompts higher sensor affectability. Subsequently, numerous systems have been received to build the particular surface

Copyright © 2019 by UOT, IRAQ

of detecting films with fine structured, taking advantage of the large specific surface of finely structured materials [11].

Spray pyrolysis technique has been carried out to a broad range of synthesis of thin and thick layers. Even multi-layered dense and porous films and powders can be readily synthesized utilizing this technique [12]. These layers were utilized in different equipment, for example, solar cells, sensors, and solid oxide fuel cells [7]. The properties of the precipitate layer depend on the conditions of fabrication [13]. Therefore, we report a technique that could successfully prepare Cr_2O_3-WO_3 composite films using a modified spray pyrolysis technique by using a dual nozzle spray system. The suggested process is easy, rapid, clean and actively efficient for the preparation of microcrystalline materials with controlled size and shape and high density of the surface area, which are suitable for technological applications such as gas sensor applications.

2. Materials and Experimental Works

I. Materials used and preparation method

The Cr_2O_3-WO_3 oxides film composites prepared using double nozzle by spray pyrolysis of aqueous solutions of tungstic acid (H_2WO_4) and chromium chloride ($CrCl_3.6H_2O$) with each solution sprayed from one nozzle, simultaneously. The molarity was (0.1 M) at three different ratios, as summarized in Table 1. The material mass was determined according to the formula ($W=M_W*V_L*M/1000$), where M_w is material molecular weight (gm/mol), M is material molarity (mol/L), V_L is distilled water volume (ml), and W is material mass (gm) [14].

Table 1: Mixing ratio of salts

Materials	Mix Ratio %		
	S1	S2	S3
H_2WO_4	3	1	1
$CrCl_3.6H_2O$	1	1	3

Silicon wafers of n-type, orientations <100> with resistivity of (0.65-0.95 Ω-cm), and (625μm) thickness used as film substrates. The silicon wafers were cut into ($1cm^2$) dimensions and dipped in diluent (1:10) HF: H_2O for (10 min) to remove native oxides layer then rinsed in ethanol for 10 min. Afterward, the substrates were washed using distilled water. Finally, they dried out by air blowing and wiped off with soft tissue.

II. Thin film deposition procedure

The entire spray system is a homemade apparatus consists of the following: heater, and thermocouple (type-k), double nozzle 1mm diameter with valve, electrical timer, air compressor, electrical gas valve and connectors.

The salts were dissolved in distilled water with a specific amount based on the molecular weight calculated according to the formula described earlier and placed on the magnetic stirrer for 20 min until the solution homogenized to ensure that the material is completely dissolved. Equal volumes of both solutions with 20 ml each sprayed simultaneously on n-type silicon substrates that heated at 500 ˚C. The deposition time procedure was (3sec) followed by (1 min) cease so that the temperature of the silicon substrates is stabilized. This procedure is controlled using electrical timer. After the end of the spraying process, all samples are left on the heater to cool down to room temperature to avoid any thermal shock that may cause a crack or distortions in the film. Other parameters such as pressure spray rate and spray distance, are listed in Table 2. After the deposition, the prepared samples were annealed for one hour at 400 ˚C and let inside the furnace until they cooled down to room temperature. This step is improving the quality and crystallinity of the films and microstructure stability [15].

Table 2: Spray system setup parameters.

Process Conditions	Value
Air pressure	6 bar
Rate of flow rate	7 cm^3/sec
Spray distance	25 ±1 cm
Spray solution size	20 ml
Feeding rate	2.5 ml/min
Spatter number	20

3. Materials Characterization

The crystal structure and phase identification of the films after annealing were characterized by x-ray diffraction (XRD) inspection with radiation CuKα (λ=1.5406 Å), The X-Ray diffraction measurements were conducted by using SHIMADZU XRD-7000 MAXima. The target is Cu beam with an angle from (10 to 60) with 40 KV & 30 mA. The microstructures of the samples were investigated by scanning electron microscopy (SEM), which is one of the most commonly used surface analysis techniques in which a wide range of scales and features can be observed. The surface roughness test was performed by using atomic force microscopy (AFM). The thickness of the prepared samples

was determined by utilizing the optical interferometer method that is depending on interference of the light beam reflected from the sample surface and substrate bottom. Laser type He-Ne (632 nm) is used, and the thickness can be obtained by using the formula below [16] and was calculated to be approximately 500 nm.

$$T = \frac{\Delta X}{X} * \frac{\lambda}{2} \quad (1)$$

Where:
T: Thickness of the film in (nm).
X: Width of fringe (cm).
ΔX: Distance between two fringes (cm).
λ: Length of wave of laser light (nm).

4. Results and Discussions

I. Crystal structure characteristics

The X-ray diffraction pattern was used to identify the phase present and its crystallite size, with 2θ° between 10 and 60. XRD analysis of all samples shows the formation of highly crystallized films. The orthorhombic tungsten oxide WO_3 and rhombohedral chromium oxide Cr_2O_3 is well indexed with the standard card of (JCPDS 20-1324) and (JCPDS 38-1479) cards respectively. The results ensure that there is no chemical interaction happened between oxides up to 600 °C, which agree with the literature [17, 18]. The sharp peak diffraction indicates the high crystallinity of the annealed oxides, and this can be attributed to the suitable preparation substrate temperature and annealing process. It is observed that no characteristic peak of impurity was detected on the XRD patterns meaning that the materials exhibit a high degree of purity, in addition to synthesis cleanness procedure.

Figure 1 presents XRD pattern of S1 and shows a mixture of WO_3 oxide as a major phase and Cr_2O_3 oxide as a minor phase due to the high content of tungsten salt. The diffraction peaks at 2θ of 23.10°, 23.70°, 24.10°, 28.78°, 33.65° and 49.33° correspond to the (001), (020), (200), (111), (201) and (400) planes, respectively, index to WO_3 oxide, and diffraction peaks at 2θ of 33.58°, 36.17°, and 54.86° correspond to the (104), (110) and (116) planes, respectively, index to Cr_2O_3 oxide. The average crystallite size was determined by the Scherrer equation [19]. Plane (001) and (104) of the WO_3 and Cr_2O_3 respectively were selected to determine the crystallite size and found to be approximately ∼15 and ∼12nm for the WO_3 and Cr_2O_3, respectively.

Figure 2 shows the XRD pattern of the sample (S2), all diffraction peaks can be readily indexed to Cr_2O_3 and WO_3 oxides, and no additional peak of other phases has been found. It could be observed increasing the diffraction peaks of Cr_2O_3 when the content of Cr salts increasing, indicates to a diffraction peaks at 2θ of 24.48°, 33.58°, 36.17°, 41.45°, and 54.86° that corresponding to the (012), (104), (110), (113) and (116) planes, respectively. While diffraction peaks at 2θ of 23.10°, 23.70°, 24.10°, 33.34°, and 41.53° that corresponding to the (001), (020), (200), (021) and (221) planes, respectively, index to WO_3 oxide. The calculated crystallite size of chosen plans (001) and (104) was ∼9 and ∼11 nm for the WO_3 and Cr_2O_3, respectively.

Figure 3 shows the XRD pattern of the sample (S3), the XRD spectra were indicated to the combination of Cr_2O_3 oxide as a major phase due to the increasing of Cr salt, and WO_3 oxide as a minor phase. The major peaks were indexed to Cr_2O_3 with diffraction peaks at 2θ of 24.48°, 33.58°, 36.17°, 41.45°, 50.22°, and 54.86° correspond to the (012), (104), (110), (113), (024) and (116) planes, respectively. While diffraction peaks at 2θ of 23.09°, 23.70° and 41.53° correspond to the (001), (020) and (221) planes, respectively, index to WO_3 oxide. The calculated crystallite size of chosen plans (001) and (104) was ∼12 and ∼14 nm for the WO_3 and Cr_2O_3, respectively.

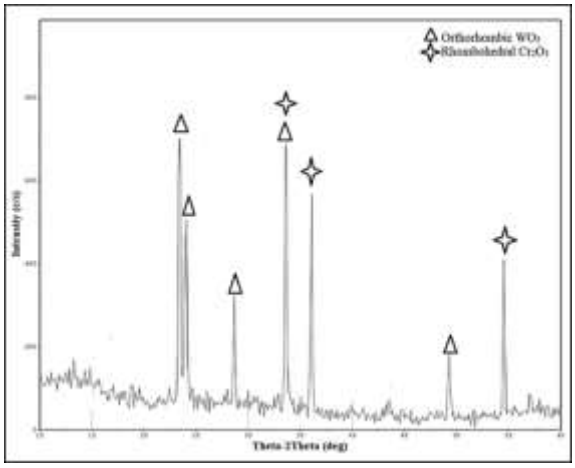

Figure1: Shows the X-ray spectra of sample (S1)

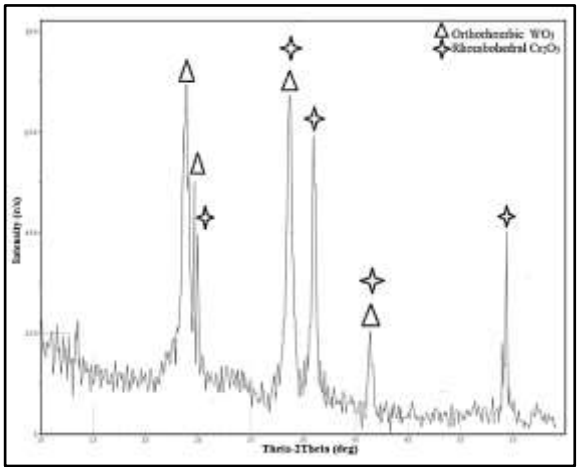

Figure 2: Shows the X-ray spectra of sample (S2).

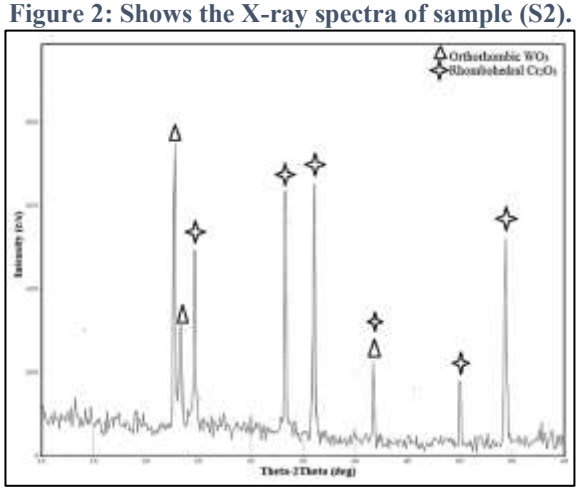

Figure 3: Shows the X-ray spectra of sample (S3)

II. Microstructural characteristics (SEM)

The morphology of the prepared samples was studied by SEM. Figures below show a microstructure of annealed samples. It is revealed that the prepared precipitate is well-crystalline formed under the current synthesis condition, which agrees well with the results of the XRD. Figure 4 shows a representative SEM image of S1, the film contain of larger grains with wide grain size range of WO_3 oxide as a major phase, could be due to the high tungsten salt used [20], while Cr_2O_3 appears as a small particle locate on faces of WO_3 grains, it is seen on a high magnification with light color. It seen that the surface of thin films is contained the small number of voids and vacancies, this is due to the method of preparation, and that is suitable for gas sensing applications, this is almost what the researchers reported [18]. Figure 5 shows a representative SEM image of sample S2, it is seen that there is an increase in agglomerates of Cr_2O_3 particles on the surface of WO_3 grains by increasing the chromium content. The microstructure showed a smaller size of Cr_2O_3 particles distributed uniformly on the WO_3 grains; it could be seen in high magnification, and this is consistent with what previous researchers have found [21]. Figure 6, shows SEM micrographs of sample S3, the microstructure of film showed a sponge morphology. It shows the surface of thin films exhibits agglomerates of WO_3 and Cr_2O_3 oxides covered the substrate surface entirely with the spherical shape at further increasing of chromium salt content; this is almost what the researchers reported by using different preparation method [18].

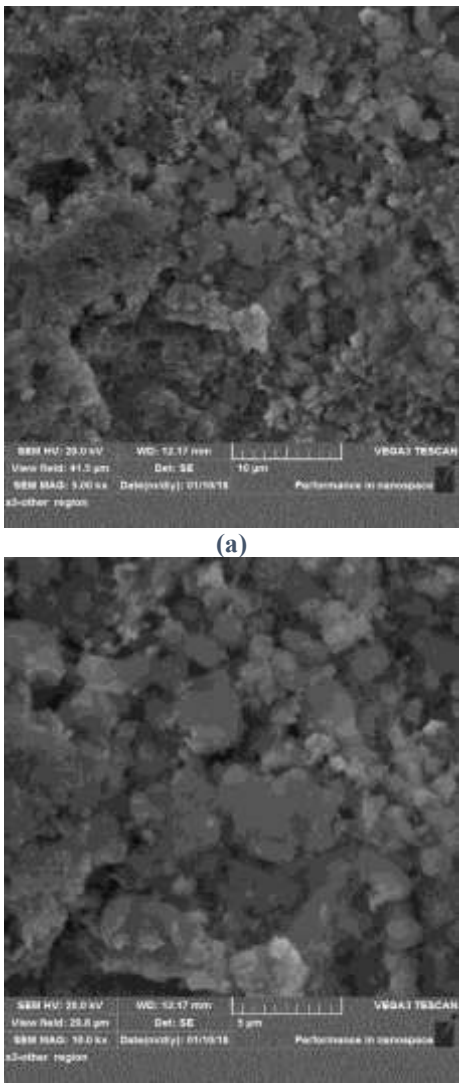

(a)

(b)

Figure 4: SEM image a) low, b) high magnification of the sample (S1)

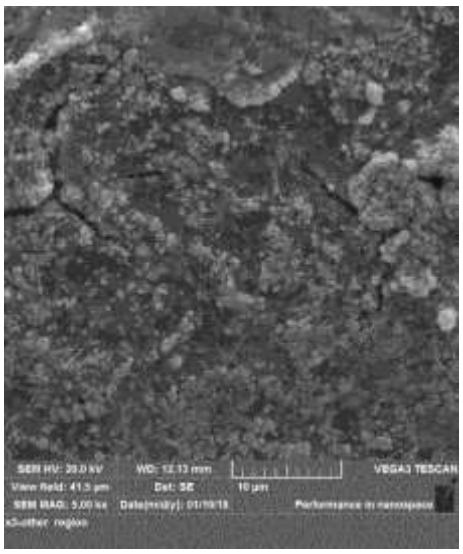

(a)

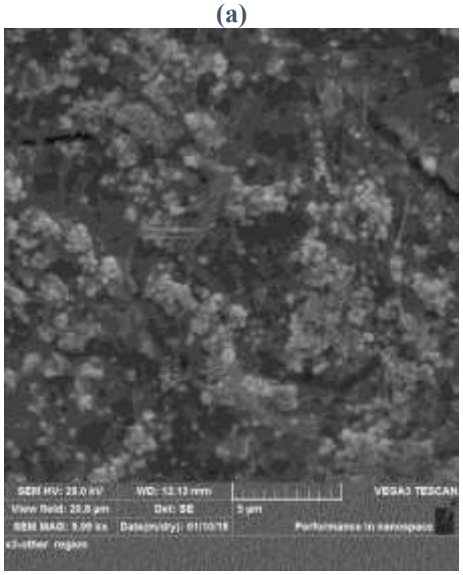

(b)

Figure 5: SEM image a) low, b) high magnification of the sample (S2)

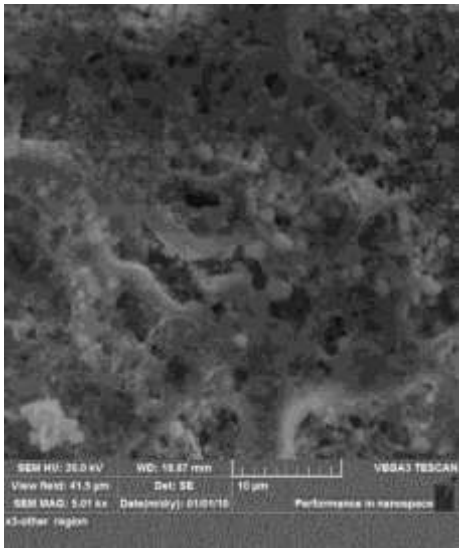

(a)

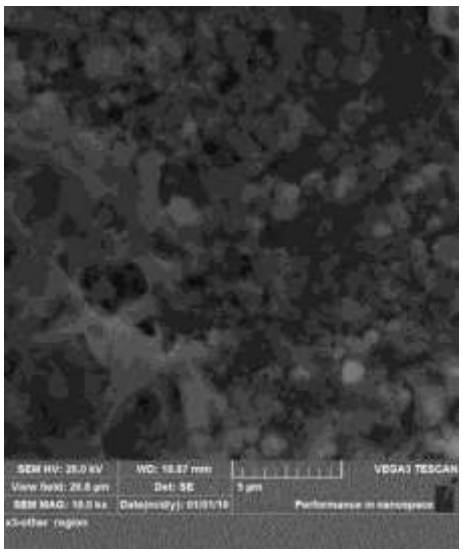

(b)

Figure 6: SEM image a) low, b) high magnification of the sample (S3)

III. Morphological characteristics (AFM)

The morphology of the samples' surface is investigated via an atomic force microscope and also used to determine the average diameter of particles of films. Figures 7-9 reveal 2D and 3D pictures after annealing at 400 °C for one hour. All films found to be well-faceted crystallites and uniformly prepared. Also, the figure shows small protrusions which cover the examined surface homogeneously, and this means that the prepared films are well deposited. Table-3 shows the variation of surface area ratio, average roughness and the average diameter of annealed samples to investigate the influence of (W: Cr) salts ratio. It is observed that: there is a difference in the roughness and the average diameter values as the chromium addition changes, and sample (S3) have the highest roughness due to the high content of Cr_2O_3 where large clusters and agglomerates spherical shape of synthesized Cr_2O_3 oxide formed. In addition, a high surface area ratio due to sponge cloud morphology contains a lot of voids and vacancies, while in samples (S1) and (S2), the microstructure consists of a fine and small size of spherical particles of Cr_2O_3 according to SEM images.

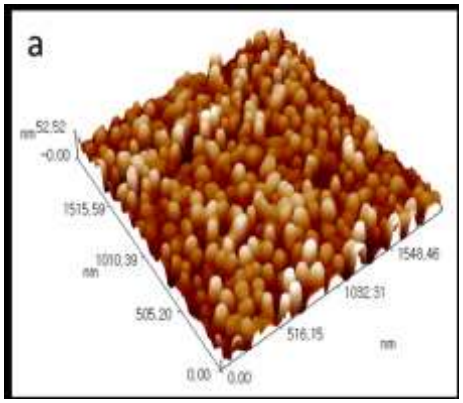

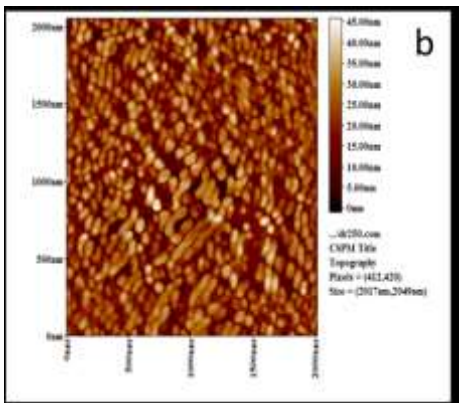

Figure 7: AFM image (a) 3D, (b) 2D of sample (S1)

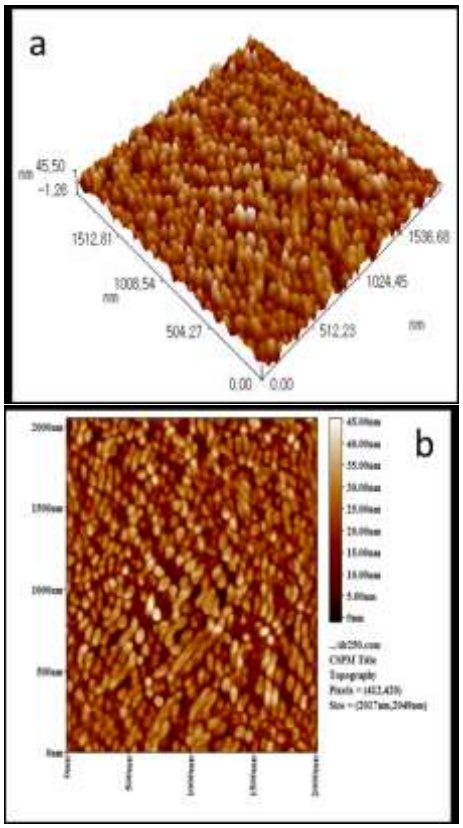

Figure 8: AFM image (a) 3D, (b) of sample (S2)

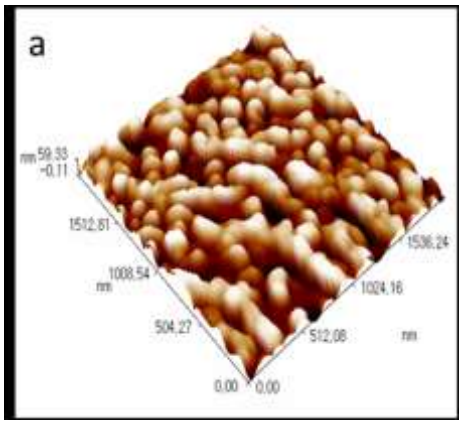

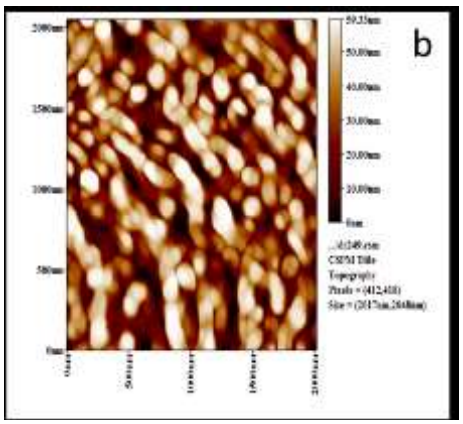

Figure 9: AFM image (a) 3D, (b) 2D of sample (S3)

4. Conclusion

1. We conclude that the spray pyrolysis technique utilizing dual nozzles and the substrate temperature is suitable to obtain crystallized Cr_2O_3/WO_3 oxides film composite.
2. Spray pyrolysis method by employed double nozzles exhibits rough and porous microstructures of Cr_2O_3/WO_3, and this type has been known as one of the most effective microstructures due to having high surface area particularly in gas detection applications
3. From XRD and SEM results, it can be concluded that the content of chromium salt influenced the phase and morphology of Cr_2O_3/WO_3 films synthesized by advanced spray pyrolysis technique. Increasing the chromium salt content has altered the shape topography and microstructure of the prepared samples.
4. From AFM results, it is concluded that the content of chromium salt influenced on the roughness values, were found that sample (S3) has the highest surface area due to the microstructure of film showed sponge morphology.

References

[1] W. Zhou, J. Huang, J. Li, Z. Xu, L. Cao, C. Yao and J. Lu., "Cr_2WO_6 nanoparticles prepared by hydrothermal assisted method with selective adsorption properties for methylene blue in water," Materials Science in Semiconductor Processing, Vol. 34, No. 1, pp. 170-174, 2015.

[2] C.M. Ghimbeu, "Preparation and Characterization of metal oxide semiconductor thin films for the detection of atmospheric pollutant gases", Ph.D thesis, Electronics Department, University Paul Verlaine of Metz, France, 2007.

[3] K. Zakrzewska, "Mixed oxides as gas sensors", Thin solid films, Vol. 391, No. 2, pp. 229-238, 2001.

[4] X. Liu, S. Cheng, H. Liu, S. Hu, D. Zhang and H. Ning, "A Survey on Gas Sensing Technology", Sensors, Vol. 12, No. 1, pp. 9635-9665, 2012.

[5] C. Sun, G. Maduraiveeran and P. Dutta, "Nitric oxide sensors using combination of p-and n-type semiconducting oxides and its application for detecting NO in human breath", Sensors and Actuators B: Chemical, Vol. 186, No. 1, pp. 117-125, 2013.

[6] Q. Zhang, M. Xu, Z Shen. and Q. Wei, "A nanostructured Cr_2O_3/WO_3 p–n junction sensor for highly sensitive detection of butanone", Journal of Materials Science: Materials in Electronics, Vol. 28, No. 16, pp. 12056-12062, 2017.

[7] K. Galatsis, Y.X. Li, W. Wlodarski, E. Comini, G. Sberveglieri, C. Cantalini, S. Santucci and M. Passacantando, "Comparison of single and binary oxide MoO_3, TiO_2 and WO_3 sol–gel gas sensors", Sensors and Actuators B: Chemical, Vol. 83, No. 3, pp. 276-280, 2002.

[8] O.J. Ilegbusi, S.N. Khatami and L.I. Trakhtenberg, "Spray Pyrolysis deposition of single and mixed oxide thin films", Materials Sciences and Applications, Vol. 8, No. 2, pp. 153-169, 2017.

[9] X. Peng, "Nanowires - Recent Advances", InTech Publisher, Croatia, Ch.1, 2012.

[10] Q. H. Wu, L. Jing and S. S. Gang, "Nano SnO2 Gas Sensors", Current Nanoscience Journal, Vol. 6, No. 5, pp. 525-538, 2010.

[11] B. Ding, M. Wang, J. Yu and G. Sun, "Gas sensors based on electrospun nanofibers", Sensors, Vol. 9, No. 3, pp. 1609-1624, 2009.

[12] D. Perednis and, L. J. Gauckler, "Thin film deposition using spray pyrolysis", Journal of electroceramics, Vol. 14, No. 2, pp. 103-111, 2005.

[13] D. Perednis: "Thin film deposition by spray pyrolysis and the application in solid oxide fuel cells", Ph.D. Thesis, Swiss Federal Institute of Technology Zurich, Lithuania, 2003.

[14] G. Baysinger and L. I. Berger, "CRC Handbook of Chemistry and Physics" CRC publication, 96th ed, National Institute of Standards and Technology, Sweden, 2003.

[15] N.V. Long, T. Teranishi, Y. Yang, C.M. Thi, Y. Cao and M. Nogami, "Iron oxide nanoparticles for next generation gas sensors", International Journal of Metallurgical & Materials Engineering, Vol. 1, No. 1, pp.1-18, 2015.

[16] M. Hernandez, A. Juarez and R. Hernandez, "Interferometric thickness determination of thin metallic films", Superficies y vacío, Vol. 9, No. 1, pp. 283-285, 1999.

[17] S. Choi, M. Bonyani, G. J. Sun, J. K. Lee, S. K. Hyun and C. Lee, "Cr_2O_3 nanoparticle-functionalized WO_3 nanorods for ethanol gas sensors", Applied Surface Science, Vol. 432, No. 1, pp. 241-249, 2018.

[18] P. Gao, H. Ji, Y. Zhou and X. Li, "Selective acetone gas sensors using porous WO_3–Cr_2O_3 thin films prepared by sol–gel method", Thin Solid Films, Vol. 520, No.7, pp. 3100-3106, 2012.

[19] H. Eranjaneya and G. T. Chandrappa, "Solution combustion synthesis of nano $ZnWO_4$ photocatalyst", Transactions of the Indian Ceramic Society, Vol. 75, No. 2, pp. 133-137, 2016.

[20] Q. Diao, C. Yin, Y. Liu, J. Li, X. Gong, X. Liang, S. Yang, H. Chen and G. Lu, "Mixed-potential-type NO_2 sensor using stabilized zirconia and Cr_2O_3–WO_3 nanocomposites", Sensors and Actuators B: Chemical, Vol. 180, No. 1, pp. 90-95, 2013.

[21] V. B. Gaikwad, G. H. Jain and R. L. Patil, "Gas Sensing Performance of Pure and Cr_2O_3 Modified WO_3 Thick Films", IEEE Sensors Conference, New Orleans, LA, USA, pp. 320-324, 2009.